catalysts

MDPI

Article

High Internal Phase Pickering Emulsion Stabilized by Lipase-Coated ZIF-8 Nanoparticles towards Recyclable Biphasic Biocatalyst

Chuanbang Xu †, Yan Sun †, Yuanyuan Sun, Ruiyun Cai and Shengmiao Zhang *

Shanghai Key Laboratory of Advanced Polymeric Materials, Key Laboratory for Ultrafine Materials of Ministry of Education, School of Materials Science and Engineering, East China University of Science and Technology, Shanghai 200237, China

* Correspondence: shmzhang@ecust.edu.cn

† These authors contributed equally to this work.

Abstract: High internal phase Pickering emulsion (Pickering HIPE) stabilized by enzyme-decorated metal-organic frameworks (MOFs) nanoparticles is developed for biphasic biocatalysts to enhance lipase catalysis and recycling. Specifically, enzyme decorated nanoparticles are prepared via ZIF-8 physisorption of a model lipase *Candida antarctica* Lipase B (CALB), named ZIF-8@CALB, to be both Pickering stabilizer and catalytic sites. An oil-in-water (o/w) Pickering HIPE with oil/water volume ratio of 3 could then be fabricated by homogenizing *p*-nitrophenyl palmitate (*p*-NPP) n-heptane solution into the ZIF-8@CALB aqueous dispersion. The biocatalytic hydrolysis of *p*-NPP is conducted by just standing the biphasic system at room temperature. The Pickering HIPE system achieves a product conversion of up to 48.9% within 0.5 h, whereas the *p*-NPP n-heptane solution system containing free CALB only achieves a stable product conversion of 6.8% for the same time. Moreover, the ZIF@CALB could be recovered by a simple centrifugation at 800 rpm, and then reused in the next cycle. The hydrolysis equilibrium conversion rate of *p*-NPP keeps over 40% for all 8 cycles, reflecting the high catalytic efficiency and recyclability of the Pickering HIPE. This study provides a new opportunity in designing Enzyme-MOFs-based Pickering interfacial biocatalyst for practical applications.

Keywords: enzyme decorated MOFs; high internal phase Pickering emulsion; interfacial biocatalysis

Citation: Xu, C.; Sun, Y.; Sun, Y.; Cai, R.; Zhang, S. High Internal Phase Pickering Emulsion Stabilized by Lipase-Coated ZIF-8 Nanoparticles towards Recyclable Biphasic Biocatalyst. *Catalysts* **2023**, *13*, 383. https://doi.org/10.3390/catal13020383

Academic Editors: Rosa María Oliart-Ros, María Guadalupe Sánchez-Otero and Evangelos Topakas

Received: 10 November 2022
Revised: 1 February 2023
Accepted: 3 February 2023
Published: 10 February 2023

1. Introduction

As natural catalysts, enzymes have excellent properties, such as high efficiency, stereoselectivity and avoiding protection or activation of functional groups during the reaction [1]. Enzymatic catalysis is one of the most important ways to realize green and sustainable industrial chemical processes [2]. However, enzymes usually have some inherent shortcomings that hinder their practical applications, such as fragile structure, low operational stability, lack of reusability, low thermal stability, and narrow pH range [3]. Immobilization techniques are proven as an attractive and efficient approach for improving enzymes structural stability and avoiding enzymes inactivity [2]. Therefore, immobilizing the enzymes on the substrate is a key strategy to improve the practical application performance of the enzymes and broaden its application fields [4]. In the past two decades, many studies have focused on the immobilization of enzymes on different substrates, such as sol-gels, organic polymers, porous and non-porous inorganic materials, etc. [5–7].

A number of nanoparticles have been investigated as substrates for immobilizing enzymes to stabilize Pickering emulsions, such as silica nanoparticles [8,9], carbon nanoparticles [10], starch nanoparticles [11] and polymeric nanoparticles [12] (Table S1). For instance, Meng et al. used a multi-step method for the synthesis of silica nanospheres [8,9], including incubation under harsh and toxic conditions. The lack of flexibility in the synthesis of silica

and carbon [10] nanoparticles and the random arrangement of pore channels in polymeric nanoparticles [12] limit their use in enzyme immobilization. As an alternative to circumventing these problems, natural macromolecules have been investigated to immobilize enzymes, such as starch nanoparticles [11], β-cyclodextrin, chitosan, and lignin colloid. However, the large and fragmented pores of natural macromolecules make it difficult to immobilize enzymes.

Recently, metal-organic frameworks (MOFs), novel porous crystalline organic-inorganic hybrid materials that consisted of metal or metal oxide corners connected by organic linkers [13], have been considered as a suitable substrate for enzyme immobilization because of their excellent physicochemical properties like polar/apolar balance, thermal stability, high surface area, tunable pore sizes and biocompatibility [14–16]. Furthermore, MOFs can protect the enzymes from the external environment, thereby improving the thermostability and chemical stability of the enzymes [17,18]. Zeolite imidazolate framework (ZIF) as a branch of MOFs is a good candidate as substrate for immobilization of enzymes due to its adjustable pore size and chemical functions [19]. Several methods including covalent bonding [20], co-precipitation [21], physical adsorption [22], and embedding [23–25] have been applied to immobilize enzymes onto MOFs [26]. For instance, Qi et al. loaded the enzyme inside a capsulate with ZIF-8 as shell prepared by a biomimetic mineralization process to achieve a Pickering interfacial system for enhanced lipase catalysis and recycling in organic media [18]. Notably, because size selectivity of the ZIF-8 shell induced different locations of the substrates in contact with the enzymes, an obvious discrepancy in catalysis efficiency was observed for substrates with different sizes. The ZIF-8 embedding method immobilizes enzymes that are selective for the size of the catalytic substrate. Covalent bonding can prevent enzymes leaching [3]. However, achieving these strong multipoint covalent linkages between the enzyme and the carrier requires more complex preparation methods than physical adsorption [27]. Enzymes that are not pretreated or chemically modified during physical adsorption can interact with MOFs through weak interactions under mild conditions, which make it ideal for preserving the structure and activity of the enzymes [22]. Nevertheless, as yet these studies have been limited to the single-phase catalysis.

Pickering interfacial catalysis (PIC), typically enabled by the use of catalytically active micro-/nanoparticles to stabilize emulsions, has been developed [28–33]. The previous works have proved that PIC is a highly efficient biphasic catalysis system. Lately, the PIC concept has been developed into Pickering interfacial biocatalysis (PIB), in which biohybrid catalyst particles prepared by integrating enzyme and its solid carriers are used as Pickering stabilizer [34]. For instance, biohybrid catalyst particles from immobilizing enzyme into/onto colloidsomes [35], polymersomes [36], MOFs [2,18], and polymer nanoparticles [12] to be Pickering stabilizer for either esterification or hydrolysis reactions at water-oil interface. PIB not only improves the reaction efficiency, but also promotes the recoverability and availability of biocatalyst after reaction. However, the practical application of PIB is limited by both the small organic/aqueous volume ratio (normally $\leq$1/1) and the instability of the Pickering emulsions [37]. From a perspective of industrial view, a highly efficient PIB system with properties of high oil/water ratio, super-stability, and recyclability is still to be developed. Whereas, it is difficult to balance the high-volume ratio, stability, and recyclability in a PIB system.

Herein, we loaded a model enzyme, *Candida antarctica* lipase B (CALB) onto ZIF-8 by physical adsorption to form ZIF-8@CALB nanoparticles (ZCPs) for stabilizing high internal phase Pickering emulsions (Pickering HIPE) with oil/water volume ratio of 3. CALB lipase can be considered as the most widely used and effective biocatalyst for amino hydrolysis reactions. And it has a high stability and enantioselectivity. The catalytic activity of CALB in aminolysis reactions with primary amines as substrates is remarkable. However, the catalytic rate and conversion of CALB were very low when the substrate was a secondary or tertiary amine [38]. HIPE is an emulsion in which the internal phase occupying more than 74 vol% [39–42]. ZIF-8 has been proved to be a suitable stabilizer for emulsion, even

HIPE [35], due to their amphiphilic feature to assemble at the liquid-liquid interface [43,44]. With the Pickering emulsion as a PIB system, we measured the catalytic hydrolysis reaction of *p*-nitrophenyl palmitate (*p*-NPP, a poorly water-soluble substrate) to explore the catalytic hydrolysis ability of ZCP. ZIF-8 was selected as the MOFs material because of its high surface area, high surface activity [45] and special chemical and thermal stability [46]. The PIB system stabilized with ZCP produced a large number of micron-sized oil droplets, which were separated from the water by the amphiphilic nature of the ZCP wrapped around the surface of the droplets. *p*-NPP dissolved in the oil phase was converted to water-soluble *p*-NP by the catalysis of ZCP, and thus entered the aqueous phase. The biocatalytic reaction proved that ZCP had high catalytic hydrolysis efficiency at the water-oil interface because of the synergistic effect of the high specific interface area of the emulsions and the high catalytic hydrolysis efficiency of the enzymes.

2. Results and Discussion

2.1. Preparation and Characterization of ZCPs

The ZCPs were prepared in two steps. ZIF-8 nanoparticles were first fabricated by the coordination of Zn^{2+} ions with 2-methylimidazole (HMIM) [44,47], and then CALB was added using a physical adsorption approach. The intensity peaks of the XRD patterns of the ZIF-8 nanoparticles were clear and sharp (Figure S1), indicating good crystallinity; and they matched well with the standard XRD pattern of ZIF-8. The SEM analysis showed that both of ZIF-8 nanoparticles and ZCPs had a uniform grained size (Figure 1). The ZIF-8 nanoparticles had an angular rhombic dodecahedral shape, while the surface of ZCP were rough. With the increase of CALB content, the angles on the surface of the nanoparticles gradually disappeared and tended to be rounded, reflecting that CALB was immobilized on the ZIF-8 nanoparticles. Jyotsana et al. demonstrated that macromolecular enzymes cannot enter the interior of MOFs through their voids [17]. This combining with the SEM images, it was clear that the CALB enzyme was immobilized by adsorption on the ZIF-8 surface.

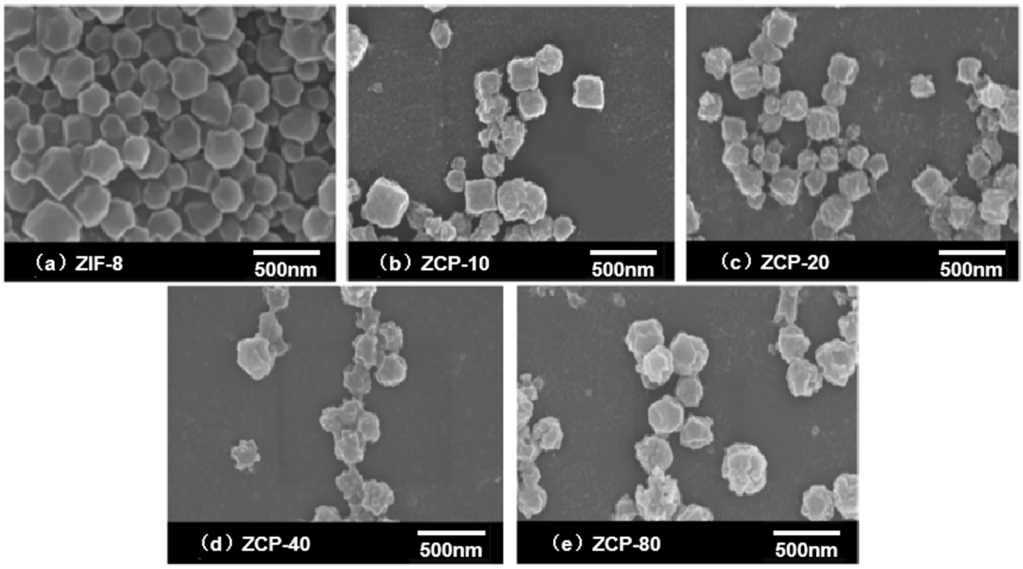

Figure 1. SEM images of ZIF-8 and ZCPs.

The content of CALB loading on the ZCP was calculated by comparing the standard concentration curve of CALB according to the BCA method (Figure S2). Table 1 summarizes the content of CALB in the ZCP and immobilization rate. As the amount of enzyme used increased, the amount of immobilized enzyme increased and the immobilization efficiency decreased.

Table 1. Enzyme Loading Capacity and Immobilization Efficiency of CALB-Loaded ZIF-8.

Sample	Enzyme Loading Capacity (μg·mg^{-1})	Immobilization Rate (%)
ZCP-10	31.6	31.6
ZCP-20	60.5	30.3
ZCP-40	97.4	24.4
ZCP-80	98.9	12.4

The successful immobilization of CALB on ZIF-8 nanoparticles was also proved by FT-IR analysis (Figure 2). The characteristic absorption peaks of ZIF-8 nanoparticles were the C=N stretching vibration at 1581 cm^{-1} and Zn-N stretching vibration at 421 cm^{-1}. For ZCPs, in addition to the characteristic absorption peaks of ZIF-8, there was an obvious absorption peak at 1625–1655 cm^{-1} which belong to the C=O stretching vibration of amide group of CALB, and the intensity of the peak increases with the increase of CALB content [48,49]. This reflected that the successfully loading of CALB on the surface of ZIF-8 nanoparticles to form ZCPs. As listed in Table S1, the immobilization rate was comparable to the case with other inorganic particles.

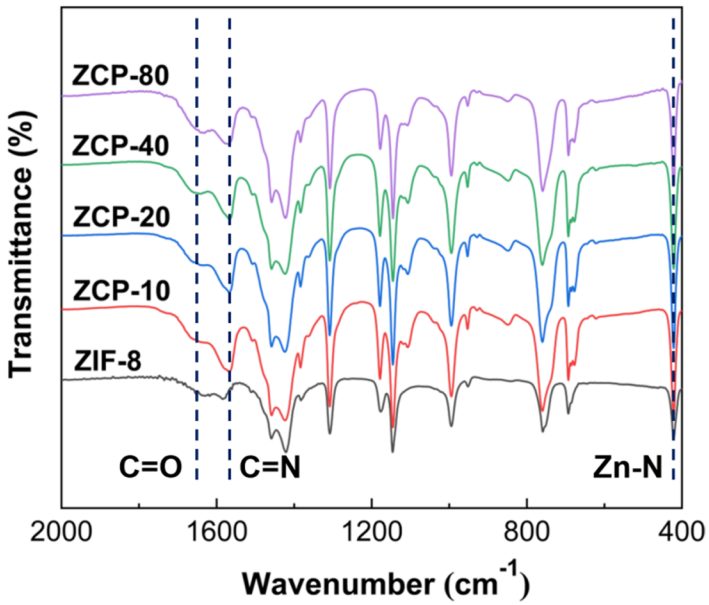

Figure 2. FT-IR spectra of ZIF-8 and ZCPs.

The water contact angles of ZCP-10, ZCP-20, ZCP-40, and ZCP-80 were 70.7 ± 2.4°, 67.5 ± 1.5°, 65.7 ± 1.2° and 63.7 ± 2.5°, respectively (Figure 3), indicating ZCPs became more hydrophilic as the amount of immobilized CALB increased. The water contact angles of the ZCPs ranged from 80° to 60°, reflecting that they could be Pickering stabilizer for oil-in-water (o/w) emulsions [50,51].

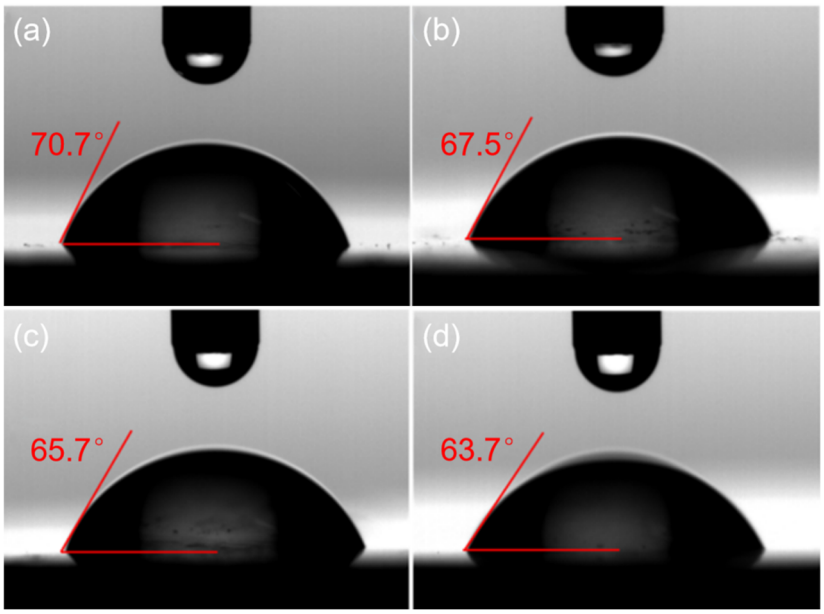

Figure 3. Air-water contact angles on CALB-loaded ZIF-8 substrates: (**a**) ZCP-10; (**b**) ZCP-20; (**c**) ZCP-40; and (**d**) ZCP-80.

2.2. Preparation of Pickering Emulsion

The confined oil droplets in o/w emulsion can be considered as an individual microreactor, which is suitable for interfacial catalyzing poorly water-soluble substrates by enlarging catalytic contact area and accelerating mass transfer. So that, a stable o/w Pickering emulsion is the basic and key precondition for achieving a high catalytic efficiency.

Microscopy analysis of the Pickering HIPEs with varied internal phase volume fraction and varied ZCP concentration showed that oil droplets were of diameter in 25–167 μm (Figure 4). The red emission from rhodamine B located in the aqueous phase confirmed that these emulsions were the type of o/w. The polyhedron n-heptane droplets were tightly surrounded by aqueous phase like a typical droplet morphology of high internal phase emulsions [42,52]. The mean droplet size increased with increasing CALB immobilization content (Figure 4a–d) and decreased with increasing ZCP concentration (Figure 4e,b,f, respectively). The mean droplet diameters were 55 ± 15 μm, 76 ± 25 μm, 113 ± 46 μm and 117 ± 50 μm, respectively, when the ZCP concentration was kept at 4.0 wt% and the emulsions were stabilized with ZCP-10, ZCP-20, ZCP-40, and ZCP-80, respectively. The prepared emulsion was named H-X-Y, where X and Y represent ZCP content in aqueous phase and the types of ZCP, respectively, as shown in Table 2. Herein, when the fixed CALB content rose in the 0.632 to 1.978 mg range (Table 1), the water contact angle of ZCP dropped between 70.7° and 63.7° (Figure 3), which reduced the stability of the Pickering emulsion and therefore resulted in bigger droplets. As reported in literature, a decrease in water contact angle of the Pickering stabilizer between 80° to 60° would reduce the stability of o/w Pickering emulsion [53].

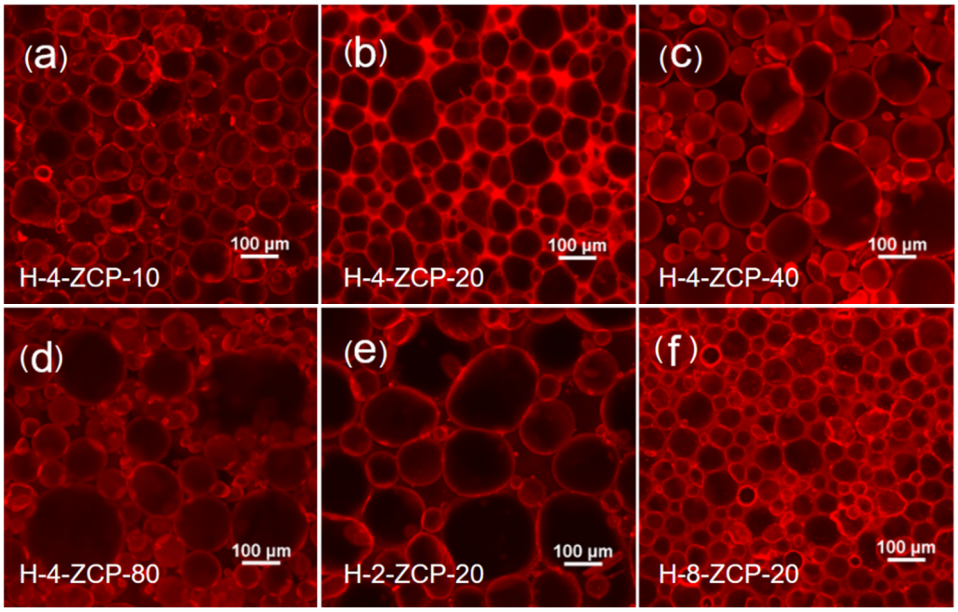

Figure 4. LSCM images of Pickering HIPEs with different ZCP kinds and concentrations: (**a**) H-4-ZCP-10; (**b**) H-4-ZCP-20; (**c**) H-4-ZCP-40; (**d**) H-4-ZCP-80; (**e**) H-2-ZCP-20; and (**f**) H-8-ZCP-20. The aqueous phase was dyed with Rhodamine B, and the emission wavelength was 561 nm.

Table 2. Composition of o/w emulsions stabilized by ZCP.

Sample	f_i (vol%) [1]	ZCP Concentration (wt%) [2]	ZCP	The Mean Droplet Diameter (μm)
H-4-ZCP-10	75	4	ZCP-10	55 ± 15
H-4-ZCP-20	75	4	ZCP-20	76 ± 25
H-4-ZCP-40	75	4	ZCP-40	113 ± 46
H-4-ZCP-80	75	4	ZCP-80	117 ± 50
H-2-ZCP-20	75	2	ZCP-20	110 ± 39
H-8-ZCP-20	75	8	ZCP-20	38 ± 13

[1] The ratio of internal phase volume to total volume; [2] The content of ZCP in the aqueous phase.

Additionally, the droplet size fell from 110 ± 39 μm to 76 ± 25 μm and 38 ± 13 μm, when the dosage of ZCP-20 was steadily raised from 2 wt% to 4 wt% and 8 wt%, respectively (Figure 4e,b,f). This was because as the concentration of ZCP increased, the number of nanoparticles per unit volume increased, which reduced the interfacial tension [54,55], and consequently smaller droplet size.

2.3. Catalytic Activity of Pickering Interfacial Biocatalysts

The Pickering interfacial biocatalytic performance of ZCP was assessed by carrying out hydrolysis of *p*-NPP in the PIB system (Figure 5). Specifically, the ZCP-20 aqueous dispersion was used as the water phase, and n-heptane containing substrate as the oil phase. Then the ZCP-20 stabilized o/w Pickering HIPE was readily formed via a homogenization. The resulting confined oil droplets provided microreaction sites, in which substrate *p*-NPP would first contact with interfacial catalysts and then convert into *p*-NP by CALB-catalyzed hydrolysis [56]. As the *p*-NP product is poor oil-solubility and good water-solubility, it would then transfer across the oil/water interface and diffuse into the aqueous phase. The *p*-NP is a yellow substance with a chromatic reaction in Pickering HIPE after mass transfer into water, as a result that the Pickering HIPE quickly changed its color from white to yellow as the *p*-NPP-catalyzed hydrolysis reaction proceeded. This process could result in

a high catalytic activity as the product moved from oil phase to aqueous phase timely once it generated, facilitating the reaction to the forward direction.

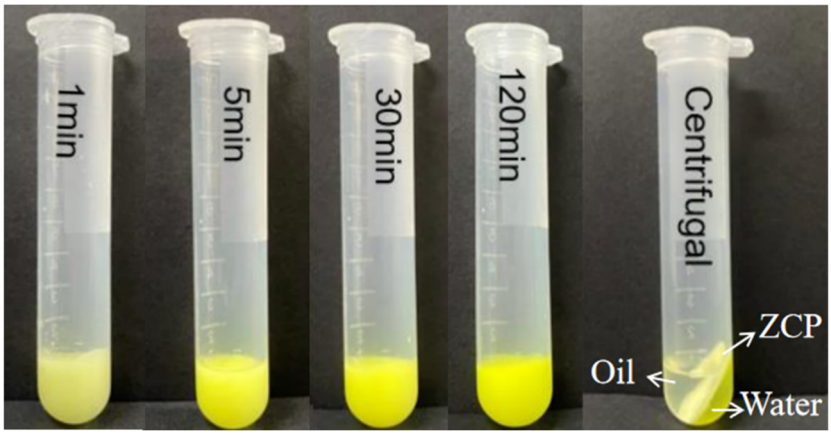

Figure 5. The degree of color development of *p*-NPP catalyzed reaction under different reaction times; after centrifugal demulsification, the water and oil phases.

The reaction can be terminated by a simple centrifugation of the emulsion into oil and aqueous phases, while the reaction substrate *p*-NPP was in the oil phase, the reaction product *p*-NP was in the aqueous phase. The upper oil phase and the lower aqueous phase were sucked separately using a dropper to ultimately extract the ZCP at the water-oil interface in a centrifuge tube as the ZCP aggregate there (Figure 5). With this technique, the catalytic nanoparticles are recovered while the reaction products are separated, making it easier to recycle the catalytic nanoparticles.

UV spectrophotometry was used to investigate the time-dependent conversion of *p*-NPP (Figure 6). As shown in Figure 6b, the hydrolysis of *p*-NPP in all four PIB systems achieved a balance conversion rate of around 50% within 1 h. Among them, the hydrolysis of *p*-NPP conducted in H-4-ZCP-20 obtained a product conversion of up to 48.9% within 0.5 h (Figure 6b). As control experiments, the hydrolysis of *p*-NPP run in both the n-heptane containing the same amount of CALB with it in H-4-ZCP-20 (Table 2) and n-heptane with ZCP-20 dispersed in it achieved a product conversion of only 6.8% and 10.4% in 0.5 h, respectively. Moreover, the later control system reached an equilibrium conversion of 20.3% in 2 h, much higher than that (10.8%) in the former control system. These results demonstrated that the immobilization of CALB to ZIF-8 improved the organic solvent resistant of the enzyme, and the PIB prepared with ZCP had a much higher catalytic efficiency than the system prepared with dispersing free CALB or ZCP in solvent. Moreover, as shown in Table S1, the catalytic activity of CALB herein is significantly higher than those with silica or carbon nanoparticles as substates, and is closer to that of commercial lipase N435 [50], indicating ZIF-8 is a good substrate for immobilization of enzyme.

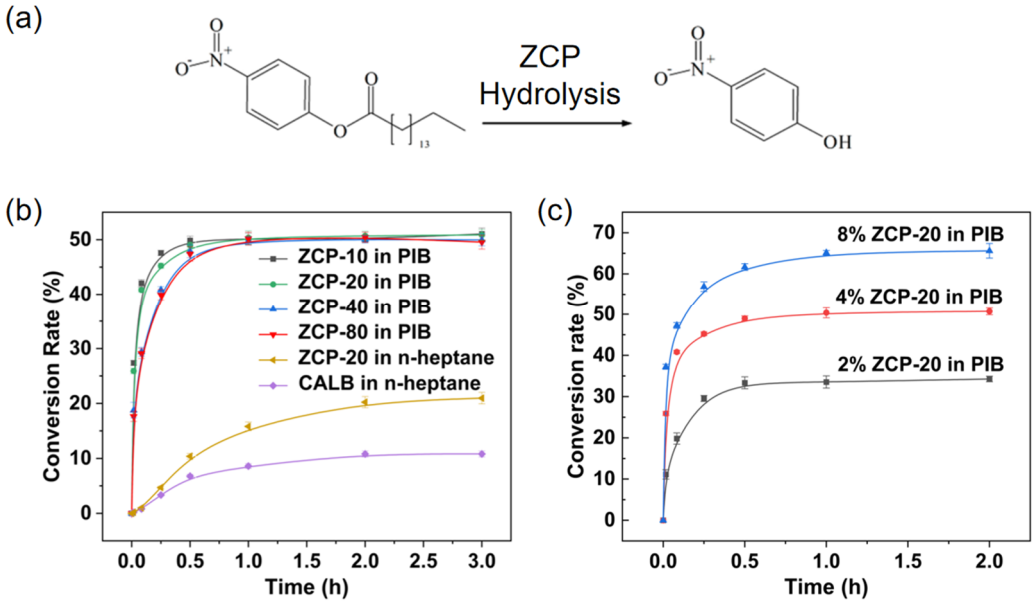

Figure 6. Interfacial biocatalytic performance for Pickering emulsion stabilized by ZCP. (**a**) The reaction of *p*-NPP hydrolysis to yield *p*-NP; (**b**) Time-dependent conversion of *p*-NPP catalyzed by different enzyme levels of ZCP in the PIB system and by CALB and ZCP-20 in the n-heptane system; (**c**) Time-dependent conversion of *p*-NPP catalyzed by different concentrations of ZCP-20 interfacial biocatalysts.

To study the nature of ZCP on the PIB efficiency, ZCP-10, ZCP-20, ZCP-40, and ZCP-80 (Table 1) were used as Pickering stabilizers to prepare Pickering emulsions with the ZCP content in the aqueous phase was kept at 4.0 wt% (Table 2). It was found that the equilibrium conversions all reached above 50% but the time to reach equilibrium conversions gradually increased (Figure 6b). This phenomenon could be owing to the decrease in the water contact angle of ZCP from 70.7° to 63.7° (Figure 3) reduced the stability of the Pickering emulsion and therefore resulted in larger droplets as shown in Figure 4 [53]. The larger droplet size, the lower interface area (and contact area between substitutes and CALB), which reduced the catalytic efficiency.

The amount of Pickering biocatalyst in the PIB was also an important fact on its catalytic efficiency. Herein, a series of Pickering HIPEs with the concentration of ZCP-20 varied between 2%, 4%, and 8% were prepared. The catalytic hydrolysis reaction of *p*-NPP was stable after 1 h and the conversion rates were 34.3%, 50.8%, and 65.6%, respectively (Figure 6c). The rate of the hydrolysis reaction also seemed to speed up (Figure 6c). As the ZCPs' content increased, the particle density per unit volume in the emulsion increased. As a result, the droplets got smaller and the surface area between the substrate and catalyst increased [57], which increased the catalytic efficiency.

Recyclability is an important performance of immobilization of enzyme for biocatalysis. To test the recyclability of the Pickering HIPE biocatalytic system, ZCP-20 was collected by centrifugation of the Pickering HIPE at 800 rpm and removal of both the oil phase and PBS buffer after the reaction. Recovered ZCP-20 was washed with PBS buffer and then n-heptane to be used for the next cycle. In the second reaction cycle, the conversion rate of *p*-NPP was 50.2%. The conversion rate was gradually decreasing in cycles 3 to 8, but was still above 40% (Figure 7), reflecting the firm immobilization of CALB onto ZIF-8. The high recyclability of the Pickering HIPE system may be due to the avoidance of enzyme shedding from the ZCP that normally caused by prolonged stirring.

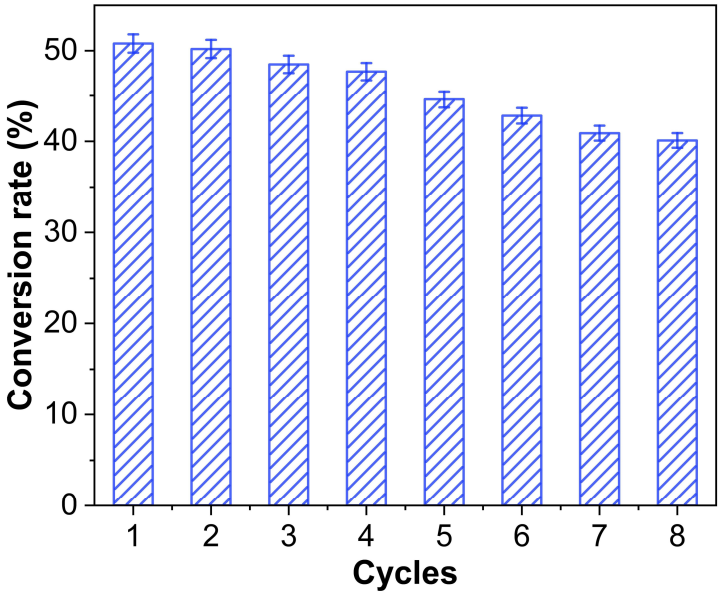

Figure 7. Recycling results of the ZCP-biocatalyzed kinetic resolution of *p*-NPP in the stirring-free Pickering HIPE system.

3. Materials and Methods

3.1. Materials

Zinc nitrate hexahydrate ($Zn(NO_3)_2 \cdot 6H_2O$, >98%), sodium chloride (NaCl, >99.5%), potassium chloride (KCl, >99.5%), potassium bromide (KBr, >99.5%), disodium hydrogen phosphate ($Na_2HPO_4 \cdot 12H_2O$, >99.5%), n-heptane (>97%) and potassium dihydrogen phosphate (KH_2PO_4, >99.5%) were purchased from Shanghai Titan Scientific Chemical Reagent Co. *p*-Nitrophenyl palmitate (*p*-NPP, >98%), 2-methylimidazole (HMIM, >99%), rhodamine B (>98%) and Lipase B from *Candida antarctica* expressed in Aspergillus (CALB, 6%) were bought from Sigma-Aldrich (Shanghai, China). Distilled water was lab made.

3.2. Methods

3.2.1. Synthesis of ZCP

ZIF-8 nanoparticles were synthesized according to the literature [58]. Briefly, Zn $(NO_3)_2 \cdot 6H_2O$ (0.744 g, 2.5 mM) in 10 mL of water was rapidly poured into 90 mL aqueous solution of HMIM (12.31 g, 150 mM) with stirring at 600 rpm for 12 h at room temperature. After the reaction, the ZIF-8 aqueous dispersion was ultrasonicated for 10 min to form a uniformly aqueous dispersion. Then various amounts (10, 20, 40 or 80 mg) of CALB were rapidly added to the ZIF-8 aqueous dispersion with stirring at 600 rpm for 2 h at room temperature, followed by two centrifugation/wash cycles (10,000 rpm, 5 min) with deionized water to obtain ZCP. Finally, the ZCP was lyophilized. The resulting ZCP with various CALB additions were named ZCP-10, ZCP-20, ZCP-40, and ZCP-80, respectively.

3.2.2. Preparation of Pickering HIPE

n-Heptane of 1.5 mL and ZCP-10 aqueous dispersion (4 wt%) of 0.5 mL were charged into a 10 mL plastic vessel at room temperature. Pickering HIPE was readily formed using an Ultra Turrax T18 homogenizer at 12,000 rpm for 30 s. The procedure was then repeated with various nanoparticles (ZCP-20, ZCP-40, and ZCP-80) and contents (2 wt%, and 8 wt%) to prepared a series of Pickering HIPEs. The prepared emulsion was named H-X-Y, where X and Y represent ZCP content in aqueous phase and the types of ZCP, respectively, as shown in Table 2.

3.2.3. Biocatalysis

Disodium hydrogen phosphate dodecahydrate (13.56 g), potassium dihydrogen phosphate (0.28 g), sodium chloride (0.8 g), and potassium chloride (0.02 g) were dissolved in 200 mL deionized water to create a PBS buffer (0.2 M, pH = 8). To prepare a PIB system, a mixture of 1.5 mL n-heptane containing 2.5 mg·mL^{-1} *p*-NPP and 0.5 mL PBS buffer containing ZCP were homogenized at 12,000 rpm for 30 s. The catalytic reaction was then conducted by simply standing the emulsion in an incubator at 40 °C. The emulsion was separated by centrifugation at 800 rpm for five minutes to end the reaction. After separation, the centrifugation, the emulsion was transfer to a three phases system with a top layer (oil phase), an intermediate layer (ZCPs rich layer), and a bottom layer (aqueous phase). ZCPs were recovered by isolated from the three layers system by removal of both the top oil phase and bottom aqueous phase, followed by washing with water and n-heptane. The washing process was as follows. The separated ZCPs were redispersed into 0.5 mL PBS buffer and then recovered by a centrifugation at 10,000 rpm for 5 min. The supernatant was added to the lower aqueous phase sucked from the separated PIB system to reduce product loss caused by incomplete separation of the PIB system. The ZCPs obtained by centrifugation were washed with the same procedure but replacing the buffer with 1.5 mL of n-hexane. The washed ZCPs were then allowed to air-dry at room temperature to be used in next cycle. The concentration of hydrolysis product *p*-NP in the water composed of the supernatant produced by water washing and the aqueous phase separated from PIB system was investigated with a UV-5800 spectrometer (Shanghai Metash Instruments Co, Ltd., Shanghai, China). The concentration was determined from the intensity at 405 nm based on the basic curve from a series of known *p*-NP content aqueous solution (Figure S3).

ZIF-8 and ZCP were observed by both transmission electron microscope (TEM, JEOL TEM-1400, Tokyo, Japan) and scanning electron microscope (SEM, Hitachi S-4800, Tokyo, Japan). 1 mg ZIF-8 nanoparticles or ZCP was dispersed in 5 mL water by sonification for 5 min. A drop of the aqueous dispersion was put on a copper grid and dried in air before observation. For TEM analysis, the dried sample on copper grid was detected directly. While for SEM observation, the dried sample on grid was placed in a vacuum ion sputterer for 60 s, and then the sample was characterization using a SEM at an accelerating voltage of 15 kV. The structure and the phase purity of ZIF-8 nanoparticles were characterized by X-ray powder diffraction (XRD, D/max2550VB/PC, Osaka, Japan). The FT-IR spectra of ZIF-8 and ZCP were detected by an FT-IR machine (Nicolet 5700, Middleton, WI, USA). For the FT-IR spectroscopy disc sample, 1 mg of nanoparticles and 0.1 g of dried potassium bromide were ground into a powder and pressed using a flat sheet press into a disc sample with dimensions of 13.0 mm in diameter and 1.5 mm in thickness.

The water contact angles of ZIF-8 nanoparticles and ZCP were determined as follows. The nanoparticles were pressed by a tablet press to form a disc sample with a diameter of 13.0 mm and a thickness around 1.0 mm. Then a water droplet of 50 μL was dropped onto the disc sample, and a contact angle goniometer (JC2000C Contact Angle Meter, Powereach Co., Shanghai, China) was used to measure the contact angle. The contact angle value was given by an average of three points of the sample.

Enzymes loading capacity of ZIF-8 were calculated by a BCA assay [59,60]. Basically, the BCA assay employed the chelation reaction between bicinchoninic acid (BCA) and Cu^+ to create a BCA-Cu^+ complex with potent RR and SERRS activity. Cu^+ was reduced by the protein in an alkaline environment. Protein content was then measured using the BCA-Cu^+ complex's 562 nm absorbance [59]. To determine the CALB content in the ZCPs, 30 mg of ZCPs was dispersed in 1 mL water by ultrasonification to obtain a ZCP aqueous dispersion. To determine the CALB content in ZCP, a homogeneous aqueous dispersion of ZIF-8 was formed by treating it with ultrasound for 10 min. The ZIF-8 aqueous dispersion was obtained by dispersing 0.5 g of ZIF-8 in 50 mL of water by ultrasonication. Then various amounts (10, 20, 40 or 80 mg) of CALB were rapidly added to the ZIF-8 aqueous dispersion with stirring at 600 rpm for 2 h at room temperature, followed by centrifugation (10,000 rpm, 10 min) to obtain ZCP and supernatant. A 20 μL of the supernatant was mixed

with 200 μL of BCA reagent. The mixture was then incubated at 37 °C for 30 min and then cooled to room temperature. The mixture was filtered through a 0.22 μm filter and then measured using a UV spectrometer (UV-5800, Metash Instruments, Shanghai, China). The change of intensity at 562 nm of the sample was used to calculate the CALB content of ZCP based on the basic curve (UV-vis vs. concentration of CALB) from a series of known CALB content aqueous solution (Figure S2).

The calculation of immobilization efficiency is based on Equation (1):

$$\text{Immobilization rate}(\%) = \frac{m - CV}{m} \cdot 100\% \quad (1)$$

where m (mg) is the total amount of CALB introduced into the solution; C (mg·mL^{-1}) and V (mL) are the CALB concentration and the volume of the supernatant, respectively.

The stability of Pickering HIPE was detected by an analyzer of concentrated liquid dispersions (Turbiscan LAB Expert, Formulation, Toulouse, France). The microstructure of Pickering HIPE was determined by a laser scanning confocal microscope (LSCM, Nikon A1R, Tokyo, Japan). Rhodamine B was dissolved in 10 mL of deionized water and sonicated for 10 min. 0.5 mL rhodamine B aqueous solution containing ZCP of 4 wt% and 1.5 mL n-heptane were added to a 10 mL centrifuge tube, and then homogenized for 30 s at 12,000 rpm using an ultra Turrax T18 homogenizer to form an emulsion. The emulsion was observed by the LSCM with a 561 nm argon ion laser used as exciting light.

4. Conclusions

In conclusion, CALB immobilized ZIF-8 nanoparticle (ZCP) was designed as both Pickering stabilizers and catalytic sites of a PIB system. In this system, a Pickering HIPE, having an oil/water volume ratio of 3, was prepared with n-heptane containing *p*-NPP as the oil phase. The Pickering HIPE provided micro-reactive sites in oil droplets where substrates *p*-NPP met interfacial catalyst ZCPs and then hydrolyzed to *p*-nitrophenol (*p*-NP). An equilibrium conversion rate of 48.9% was achieved within 0.5 h, with was much higher than that (6.8%) of the hydrolysis reaction conducted in a heptane containing free CALB in 0.5 h. The ZCPs in the PIB system could be easily recovered by a simple centrifugation of the Pickering HIPE, and then reused in the next biocatalytic reaction cycle. PIB system maintained about 80% residual activity after 8 reaction cycles, reflecting the high catalytic efficiency and recyclability of ZCPs. This approach opens the door to the development of an enzyme-MOFs nanoparticle-stabilized emulsion with high oil/water volume ratio, stability, and recyclability for sustainable applications in biphasic enzyme catalysis.

Supplementary Materials: The following supporting information can be downloaded at: https://www.mdpi.com/article/10.3390/catal13020383/s1, Figure S1: XRD pattern of ZIF-8 nanoparticles, Figure S2: Standard curve of CALB concentration (0.2 M, pH = 8 PBS buffer), Figure S3: Standard curve of *p*-NP concentration (0.2 M, pH = 8 PBS buffer), Table S1: The enzyme immobilization rate and catalytic properties of immobilizing enzymes onto different kinds of particles. References [9,10,61] are cited in the supplementary materials.

Author Contributions: Original draft preparation, C.X. and Y.S. (Yan Sun); Writing—review and editing, C.X., Y.S. (Yan Sun), Y.S. (Yuanyuan Sun), R.C. and S.Z.; Supervision, S.Z. All authors have read and agreed to the published version of the manuscript.

Funding: This work was supported by the National Natural Science Foundation of China (51773059).

Data Availability Statement: Not applicable.

Conflicts of Interest: The authors declare no conflict of interest.

References

1. Li, M.; Qiao, S.; Zheng, Y.; Andaloussi, Y.H.; Li, X.; Zhang, Z.; Li, A.; Cheng, P.; Ma, S.; Chen, Y. Fabricating Covalent Organic Framework Capsules with Commodious Microenvironment for Enzymes. *J. Am. Chem. Soc.* **2020**, *142*, 6675–6681. [CrossRef] [PubMed]
2. Shi, J.; Wang, X.; Zhang, S.; Tang, L.; Jiang, Z. Enzyme-conjugated ZIF-8 particles as efficient and stable Pickering interfacial biocatalysts for biphasic biocatalysis. *J. Mater. Chem. B* **2016**, *4*, 2654–2661. [CrossRef] [PubMed]
3. Du, Y.; Gao, J.; Zhou, L.; Ma, L.; He, Y.; Huang, Z.; Jiang, Y. Enzyme nanocapsules armored by metal-organic frameworks: A novel approach for preparing nanobiocatalyst. *Chem. Eng. J.* **2017**, *327*, 1192–1197. [CrossRef]
4. Arana-Pena, S.; Carballares, D.; Morellon-Sterlling, R.; Berenguer-Murcia, A.; Alcantara, A.R.; Rodrigues, R.C.; Fernandez-Lafuente, R. Enzyme co-immobilization: Always the biocatalyst designers' choice... or not? *Biotechnol. Adv.* **2021**, *51*, 107584. [CrossRef] [PubMed]
5. Basso, A.; Serban, S. Industrial applications of immobilized enzymes—A review. *Mol. Catal.* **2019**, *479*, 110607. [CrossRef]
6. Zhang, Y.; Ma, S. Controllable immobilization of enzymes in metal-organic frameworks for biocatalysis. *Chem. Catal.* **2021**, *1*, 20–22. [CrossRef]
7. Wang, M.; Wang, M.; Zhu, Y.; Zhang, S.; Chen, J. Enzyme immobilized millimeter-sized polyHIPE beads with easy separability and recyclability. *React. Chem. Eng.* **2019**, *4*, 1136–1144. [CrossRef]
8. Meng, T.; Bai, R.; Wang, W.; Yang, X.; Guo, T.; Wang, Y. Enzyme-Loaded Mesoporous Silica Particles with Tuning Wettability as a Pickering Catalyst for Enhancing Biocatalysis. *Catalysts* **2019**, *9*, 78. [CrossRef]
9. Luna, C.; Gascón-Pérez, V.; López-Tenllado, F.J.; Bautista, F.M.; Verdugo-Escamilla, C.; Aguado-Deblas, L.; Calero, J.; Romero, A.A.; Luna, D.; Estévez, R. Enzymatic Production of Ecodiesel by Using a Commercial Lipase CALB, Immobilized by Physical Adsorption on Mesoporous Organosilica Materials. *Catalysts* **2021**, *11*, 1350. [CrossRef]
10. Dong, Z.; Liu, Z.; Shi, J.; Tang, H.; Xiang, X.; Huang, F.; Zheng, M. Carbon Nanoparticle-Stabilized Pickering Emulsion as a Sustainable and High-Performance Interfacial Catalysis Platform for Enzymatic Esterification/Transesterification. *ACS Sustain. Chem. Eng.* **2019**, *7*, 7619–7629. [CrossRef]
11. Qi, L.; Zhou, Y.J.; Luo, Z.G.; Gao, Q.Y.; Shi, Y.C. Facile synthesis of lipase-loaded starch nanoparticles as recyclable biocatalyst in Pickering interfacial systems. *Carbohydr. Polym.* **2023**, *299*, 11. [CrossRef]
12. Wang, M.; Wang, M.; Zhang, S.; Chen, J. Pickering gel emulsion stabilized by enzyme immobilized polymeric nanoparticles: A robust and recyclable biocatalyst system for biphasic catalysis. *React. Chem. Eng.* **2019**, *4*, 1459–1465. [CrossRef]
13. Zhao, Z.; Lin, T.; Liu, W.; Hou, L.; Ye, F.; Zhao, S. Colorimetric detection of blood glucose based on GOx@ZIF-8@Fe-polydopamine cascade reaction. *Spectrochim Acta A Mol. Biomol. Spectrosc.* **2019**, *219*, 240–247. [CrossRef] [PubMed]
14. Zhou, M.; Yan, L.; Chen, H.; Ju, X.; Zhou, Z.; Li, L. Development of functionalized metal–organic frameworks immobilized cellulase with enhanced tolerance of aqueous-ionic liquid media for saccharification of bagasse. *Fuel* **2021**, *304*, 121484. [CrossRef]
15. Banerjee, R.; Phan, A.; Wang, B.; Knobler, C.; Furukawa, H.; O'Keeffe, M.; Yaghi, O.M. High-throughput synthesis of zeolitic imidazolate frameworks and application to CO2 capture. *Science* **2008**, *319*, 939–943. [CrossRef] [PubMed]
16. Wang, S.; Fan, Y.; Jia, X. Sodium dodecyl sulfate-assisted synthesis of hierarchically porous ZIF-8 particles for removing mercaptan from gasoline. *Chem. Eng. J.* **2014**, *256*, 14–22. [CrossRef]
17. Mehta, J.; Bhardwaj, N.; Bhardwaj, S.K.; Kim, K.-H.; Deep, A. Recent advances in enzyme immobilization techniques: Metal-organic frameworks as novel substrates. *Coord. Chem. Rev.* **2016**, *322*, 30–40. [CrossRef]
18. Qi, L.; Luo, Z.; Lu, X. Biomimetic Mineralization Inducing Lipase–Metal–Organic Framework Nanocomposite for Pickering Interfacial Biocatalytic System. *ACS Sustain. Chem. Eng.* **2019**, *7*, 7127–7139. [CrossRef]
19. Fu, H.; Ou, P.; Zhu, J.; Song, P.; Yang, J.; Wu, Y. Enhanced Protein Adsorption in Fibrous Substrates Treated with Zeolitic Imidazolate Framework-8 (ZIF-8) Nanoparticles. *ACS Appl. Nano Mater.* **2019**, *2*, 7626–7636. [CrossRef]
20. Nowroozi-Nejad, Z.; Bahramian, B.; Hosseinkhani, S. Efficient immobilization of firefly luciferase in a metal organic framework: Fe-MIL-88(NH2) as a mighty support for this purpose. *Enzyme Microb. Technol.* **2019**, *121*, 59–67. [CrossRef]
21. Inagaki, M.; Hiratake, J.; Nishioka, T.; Oda, J. One-Pot Synthesis Of Optically-Active Cyanohydrin Acetates from Aldehydes Via Lipase-Catalyzed Kinetic Resolution Coupled with Insitu Formation and Racemization Of Cyanohydrins. *J. Org. Chem.* **1992**, *57*, 5643–5649. [CrossRef]
22. Nobakht, N.; Faramarzi, M.A.; Shafiee, A.; Khoobi, M.; Rafiee, E. Polyoxometalate-metal organic framework-lipase: An efficient green catalyst for synthesis of benzyl cinnamate by enzymatic esterification of cinnamic acid. *Int. J. Biol. Macromol.* **2018**, *113*, 8–19. [CrossRef] [PubMed]
23. Dai, D.Z.; Xia, L.M. Effect of lipase immobilization on resolution of (R, S)-2-octanol in nonaqueous media using modified ultrastable-Y molecular sieve as support. *Appl. Biochem. Biotechnol.* **2006**, *134*, 39–50. [CrossRef] [PubMed]
24. Kim, J.; Jia, H.F.; Wang, P. Challenges in biocatalysis for enzyme-based biofuel cells. *Biotechnol. Adv.* **2006**, *24*, 296–308. [CrossRef] [PubMed]
25. Ispas, C.; Sokolov, I.; Andreescu, S. Enzyme-functionalized mesoporous silica for bioanalytical applications. *Anal. Bioanal. Chem.* **2009**, *393*, 543–554. [CrossRef]
26. Beh, J.J.; Lim, J.K.; Ng, E.P.; Ooi, B.S. Synthesis and size control of zeolitic imidazolate framework-8 (ZIF-8): From the perspective of reaction kinetics and thermodynamics of nucleation. *Mater. Chem. Phys.* **2018**, *216*, 393–401. [CrossRef]

27. Mateo, C.; Palomo, J.M.; Fernandez-Lorente, G.; Guisan, J.M.; Fernandez-Lafuente, R. Improvement of enzyme activity, stability and selectivity via immobilization techniques. *Enzyme Microb. Technol.* **2007**, *40*, 1451–1463. [CrossRef]
28. Pera-Titus, M.; Leclercq, L.; Clacens, J.M.; De Campo, F.; Nardello-Rataj, V. Pickering interfacial catalysis for biphasic systems: From emulsion design to green reactions. *Angew. Chem.* **2015**, *54*, 2006–2021. [CrossRef]
29. Xi, Y.; Liu, B.; Wang, S.; Huang, X.; Jiang, H.; Yin, S.; Ngai, T.; Yang, X. Growth of Au nanoparticles on phosphorylated zein protein particles for use as biomimetic catalysts for cascade reactions at the oil–water interface. *Chem. Sci.* **2021**, *12*, 3885–3889. [CrossRef]
30. Chang, F.; Vis, C.M.; Ciptonugroho, W.; Bruijnincx, P.C.A. Recent developments in catalysis with Pickering Emulsions. *Green Chem.* **2021**, *23*, 2575–2594. [CrossRef]
31. Bago Rodriguez, A.M.; Schober, L.; Hinzmann, A.; Groger, H.; Binks, B.P. Effect of Particle Wettability and Particle Concentration on the Enzymatic Dehydration of n-Octanaloxime in Pickering Emulsions. *Angew. Chem.* **2021**, *60*, 1450–1457. [CrossRef] [PubMed]
32. Li, D.D.; Jiang, J.Z.; Cai, C. Palladium nanoparticles anchored on amphiphilic Janus-type cellulose nanocrystals for Pickering interfacial catalysis. *Chem. Commun.* **2020**, *56*, 9396–9399. [CrossRef] [PubMed]
33. Ni, L.; Yu, C.; Wei, Q.B.; Liu, D.M.; Qiu, J.S. Pickering Emulsion Catalysis: Interfacial Chemistry, Catalyst Design, Challenges, and Perspectives. *Angew. Chem.-Int. Edit.* **2022**, *61*, 24. [CrossRef]
34. Xie, H.; Zhao, W.; Ali, D.C.; Zhang, X.; Wang, Z. Interfacial biocatalysis in bacteria-stabilized Pickering emulsions for microbial transformation of hydrophobic chemicals. *Catal. Sci. Technol.* **2021**, *11*, 2816–2826. [CrossRef]
35. Jiang, H.; Hu, X.; Li, Y.; Yang, C.; Ngai, T. Engineering proteinaceous colloidosomes as enzyme carriers for efficient and recyclable Pickering interfacial biocatalysis. *Chem. Sci.* **2021**, *12*, 12463–12467. [CrossRef] [PubMed]
36. Wang, Z.; van Oers, M.C.; Rutjes, F.P.; van Hest, J.C. Polymersome colloidosomes for enzyme catalysis in a biphasic system. *Angew. Chem.* **2012**, *51*, 10746–10750. [CrossRef] [PubMed]
37. Sun, Z.; Glebe, U.; Charan, H.; Boker, A.; Wu, C. Enzyme-Polymer Conjugates as Robust Pickering Interfacial Biocatalysts for Efficient Biotransformations and One-Pot Cascade Reactions. *Angew. Chem.* **2018**, *57*, 13810–13814. [CrossRef]
38. Lima, R.N.; dos Anjos, C.S.; Orozco, E.V.M.; Porto, A.L.M. Versatility of Candida antarctica lipase in the amide bond formation applied in organic synthesis and biotechnological processes. *Mol. Catal.* **2019**, *466*, 75–105. [CrossRef]
39. Zhang, S.M.; Chen, J.D. PMMA based foams made via surfactant-free high internal phase emulsion templates. *Chem. Commun.* **2009**, *16*, 2217–2219. [CrossRef]
40. Bago Rodriguez, A.M.; Binks, B.P. High internal phase Pickering emulsions. *Curr. Opin. Colloid Interface Sci.* **2022**, *57*, 101556. [CrossRef]
41. Silverstein, M.S. PolyHIPEs: Recent advances in emulsion-templated porous polymers. *Prog. Polym. Sci.* **2014**, *39*, 199–234. [CrossRef]
42. Cameron, N.R. High internal phase emulsion templating as a route to well-defined porous polymers. *Polymer* **2005**, *46*, 1439–1449. [CrossRef]
43. Lyu, F.J.; Zhang, Y.F.; Zare, R.N.; Ge, J.; Liu, Z. One-Pot Synthesis of Protein-Embedded Metal-Organic Frameworks with Enhanced Biological Activities. *Nano Lett.* **2014**, *14*, 5761–5765. [CrossRef] [PubMed]
44. Sun, Y.; Zhu, Y.; Zhang, S.; Binks, B.P. Fabrication of Hierarchical Macroporous ZIF-8 Monoliths Using High Internal Phase Pickering Emulsion Templates. *Langmuir ACS J. Surf. Colloids* **2021**, *37*, 8435–8444. [CrossRef]
45. Bian, Z.; Zhang, S.; Zhu, X.; Li, Y.; Liu, H.; Hu, J. In situ interfacial growth of zeolitic imidazolate framework (ZIF-8) nanoparticles induced by a graphene oxide Pickering emulsion. *RSC Adv.* **2015**, *5*, 31502–31505. [CrossRef]
46. Park, K.S.; Ni, Z.; Cote, A.P.; Choi, J.Y.; Huang, R.D.; Uribe-Romo, F.J.; Chae, H.K.; O'Keeffe, M.; Yaghi, O.M. Exceptional chemical and thermal stability of zeolitic imidazolate frameworks. *Proc. Natl. Acad. Sci. USA* **2006**, *103*, 10186–10191. [CrossRef]
47. Pan, Y.; Liu, Y.; Zeng, G.; Zhao, L.; Lai, Z. Rapid synthesis of zeolitic imidazolate framework-8 (ZIF-8) nanocrystals in an aqueous system. *Chem. Commun.* **2011**, *47*, 2071–2073. [CrossRef]
48. Xing, X.; Jia, J.Q.; Zhang, J.F.; Zhou, Z.W.; Li, J.; Wang, N.; Yu, X.Q. CALB Immobilized onto Magnetic Nanoparticles for Efficient Kinetic Resolution of Racemic Secondary Alcohols: Long-Term Stability and Reusability. *Molecules* **2019**, *24*, 490. [CrossRef]
49. Chiaradia, V.; Soares, N.S.; Valerio, A.; de Oliveira, D.; Araujo, P.H.; Sayer, C. Immobilization of Candida antarctica Lipase B on Magnetic Poly(Urea-Urethane) Nanoparticles. *Appl. Biochem. Biotechnol.* **2016**, *180*, 558–575. [CrossRef]
50. Kaptay, G. On the equation of the maximum capillary pressure induced by solid particles to stabilize emulsions and foams and on the emulsion stability diagrams. *Colloids Surf. A Physicochem. Eng. Asp.* **2006**, *282–283*, 387–401. [CrossRef]
51. Horozov, T. Foams and foam films stabilised by solid particles. *Curr. Opin. Colloid Interface Sci.* **2008**, *13*, 134–140. [CrossRef]
52. Zhu, H.; Zhang, M.; Zhang, S. Preparation of Macroporous Polymers from Microcapsule-Stabilized Pickering High Internal Phase Emulsions. *Langmuir ACS J. Surf. Colloids* **2019**, *35*, 9504–9512. [CrossRef] [PubMed]
53. Binks, B.P.; Lumsdon, S.O. Influence of Particle Wettability on the Type and Stability of Surfactant-Free Emulsions. *Langmuir ACS J. Surf. Colloids* **2000**, *16*, 8622–8631. [CrossRef]
54. Wang, W.; Zhou, Z.; Nandakumar, K.; Xu, Z.; Masliyah, J.H. Effect of charged colloidal particles on adsorption of surfactants at oil-water interface. *J. Colloid Interface Sci.* **2004**, *274*, 625–630. [CrossRef]
55. Ma, H.; Luo, M.; Dai, L.L. Influences of surfactant and nanoparticle assembly on effective interfacial tensions. *Phys. Chem. Chem. Phys.* **2008**, *10*, 2207–2213. [CrossRef] [PubMed]

56. Jiang, Y.; Liu, H.; Wang, L.; Zhou, L.; Huang, Z.; Ma, L.; He, Y.; Shi, L.; Gao, J. Virus-like organosilica nanoparticles for lipase immobilization: Characterization and biocatalytic applications. *Biochem. Eng. J.* **2019**, *144*, 125–134. [CrossRef]
57. Hua, Y.; Zhang, S.M.; Zhu, Y.; Chu, Y.Q.; Chen, J.D. Hydrophilic polymer foams with well-defined open-cell structure prepared from pickering high internal phase emulsions. *J. Polym. Sci. Pol. Chem.* **2013**, *51*, 2181–2187. [CrossRef]
58. Zhang, H.F.; Zhao, M.; Lin, Y.S. Stability of ZIF-8 in water under ambient conditions. *Microporous Mesoporous Mat.* **2019**, *279*, 201–210. [CrossRef]
59. Chen, L.; Yu, Z.; Lee, Y.; Wang, X.; Zhao, B.; Jung, Y.M. Quantitative evaluation of proteins with bicinchoninic acid (BCA): Resonance Raman and surface-enhanced resonance Raman scattering-based methods. *Analyst* **2012**, *137*, 5834–5838. [CrossRef]
60. Cortes-Rios, J.; Zarate, A.M.; Figueroa, J.D.; Medina, J.; Fuentes-Lemus, E.; Rodriguez-Fernandez, M.; Aliaga, M.; Lopez-Alarcon, C. Protein quantification by bicinchoninic acid (BCA) assay follows complex kinetics and can be performed at short incubation times. *Anal. Biochem.* **2020**, *608*, 113904. [CrossRef]
61. Kowalczykiewicz, D.; Szymańska, K.; Gillner, D.; Jarzębski, A.B. Rotating bed reactor packed with heterofunctional structured silica-supported lipase. Developing an effective system for the organic solvent and aqueous phase reactions. *Microporous Mesoporous Mat.* **2021**, *312*. [CrossRef]